

Article

The Influence of the Heat Transfer Mode on the Stability of Foam Extinguishing Agents

Xia Zhou ^{1,2,*} , Zhihao An ¹, Ziheng Liu ¹, Hongjie Ha ¹, Yixuan Li ¹ and Renming Pan ¹

¹ School of Chemistry and Chemical Engineering, Nanjing University of Science and Technology, Nanjing 210094, China; anzhihao0107@njjust.edu.cn (Z.A.); liuziheng0821@njjust.edu.cn (Z.L.); hahongjie@njjust.edu.cn (H.H.); lyx2971@njjust.edu.cn (Y.L.); panrenming@njjust.edu.cn (R.P.)

² School of Fashion and Textiles, The Hong Kong Polytechnic University, Kowloon 999077, Hong Kong, China

* Correspondence: zhouxia@njjust.edu.cn; Tel./Fax: +86-025-84303159

Abstract: The mass loss mechanisms of an aqueous film-forming foam (AF foam), an AR/AFFF water-soluble film-forming foam extinguishing agent (AR foam), and a Class A foam extinguishing agent (A foam) at different levels of thermal radiation, thermal convection, and heat conduction intensity were studied. At a relatively low thermal radiation intensity, the liquid separation rate of the AF, AR, and A foams is related to the properties of the foam itself, such as viscosity and surface/interface tension, which are relatively independent of the external radiation heat flux of the foam. At low radiation intensity (15 kW/m² and 25 kW/m²), the liquid separation rate of the AF and A foams is relatively stable. When the heat flux intensity is 35 kW/m², the liquid separation rate of the AF and A foams increases notably, which may be mainly due to the rapid decrease in foam viscosity. And the mass loss behavior is dominated by liquid separation in the AF, AR, and A foams under the influence of thermal radiation and thermal convection. Under the same experimental conditions, the liquid separation rate of AF is the fastest. There is no significant difference in the evaporation rates of the three kinds of foam in the same heat conduction condition. In addition, the AR and A foams usually have a 25% longer liquid separation time (t) under thermal radiation and thermal convection, and the thermal stability is better than AF foam. The temperature reached by the AF foam layer under thermal convection was lower than that of the AR and A foams, and the time for the foam layer to reach the highest temperature under heat conduction was longer than that of the AR and A foams.

Keywords: foam extinguishing agent; heat transfer mode; stability; liquid separation; evaporate



Citation: Zhou, X.; An, Z.; Liu, Z.; Ha, H.; Li, Y.; Pan, R. The Influence of the Heat Transfer Mode on the Stability of Foam Extinguishing Agents. *Fire* **2024**, *7*, 137. <https://doi.org/10.3390/fire7040137>

Academic Editors: Grant Williamson, Jinlong Zhao, Qian Li, Jin Lin, Mingjun Xu and Youjie Sheng

Received: 23 February 2024

Revised: 30 March 2024

Accepted: 11 April 2024

Published: 12 April 2024



Copyright: © 2024 by the authors. Licensee MDPI, Basel, Switzerland. This article is an open access article distributed under the terms and conditions of the Creative Commons Attribution (CC BY) license (<https://creativecommons.org/licenses/by/4.0/>).

1. Introduction

Foam fire extinguishing agents have excellent fire extinguishing performance and are the most common type of fire extinguishing agent in fire rescue teams, petrochemical enterprises, and substations. According to the classification of different fire extinguishing objects, there are mainly synthetic foam extinguishing agents used to extinguish solid fire, and fluoroprotein and water-formed foam extinguishing agents used to extinguish oil fire [1–4]. The aqueous film-forming foam solution (AFFF) takes a fluorine surfactant as the main raw material, and also includes a hydrocarbon surfactant, a foam stabilizer, antifreeze, and other additives. By forming water film on the fuel surface and the critical point of air, it spreads rapidly on the fuel surface due to its extremely low surface tension. Water-film-forming foam forms a dense foam layer on the fuel surface to isolate oxygen and spread quickly to extinguish the fire quickly. It has strong stability, can inhibit the volatilization of liquid fuel and prevent re-ignition, and is used for preventing and fighting water-insoluble flammable and combustible liquid fires such as crude oil, petroleum, diesel oil, and aviation fuel [5–8]. The liquid separation and evaporation of foam, that is, the stability of foam extinguishing agents, are very important for the performance improvement and efficient application of foam extinguishing agents.

The stability of foam refers to the difficulty of foam bursting. Relevant research on the stability of foam extinguishing agents has been carried out [5,9–16]. The effects of nano-additives and polymers with different foam stabilizers on the properties of water-formed foam were studied, and the characteristics of liquid separation were measured [17–22]. Under the condition of thermal radiation, the mixing ratio and foaming agent type indeed affect the foam stability, and a small amount of fluoroprotein foam significantly improves the liquid separation time of mixed water-formed foam and reduces the rate of decline in foam height [23]. The increase in the NaCMC polymer concentration reduces the high attenuation of foam produced by CTAB/501W surfactant solutions, delays the process of bubble coarsening and drainage, and leads to the enhancement of foam stability [24]. Moreover, adding carboxy methyl cellulose sodium (CS) and Xanthan Gum (XG) to AFFF can slow down the foam drainage, while adding lauryl alcohol (LA) can accelerate the foam drainage [25]. From the analysis of foam coarsening and coalescence, adding a microbial polysaccharide can slow down the coarsening speed of foam and prevent foam coalescence. Diutan gum molecules have rod-like spiral structure and complex aggregation morphology, which gives diutan gum good temperature resistance and excellent water retention [26]. These two characteristics of diutan gum significantly improve its foam stability. Therefore, changes in the surface tension, viscosity, and liquid fraction of foam are the main reason for the change in the foam drainage rate [26]. It can be seen that previous research mainly focused on measures to improve the thermal stability of foam, but lacked focus on the change characteristics of the stability behavior of foam extinguishing agents [27–30]. The application scenarios of foam extinguishing agents are complex, and the thermal factors in fire scenarios seriously affect foam rupture and its stability. Therefore, it is of great guiding significance to explore the change characteristics of the stability behavior of foam extinguishing agents in thermal environments for the practical application of foam extinguishing agents. It is also helpful to develop a foam extinguishing agent with high stability in thermal environments.

Therefore, three different types of commercial foam extinguishing agents were selected to study the mass loss of foam extinguishing agents under different heat transfer methods, and the changes in height and temperature of various foam extinguishing agents were explored in this work. Then, the stability of the three foam extinguishing agents in a thermal environment was compared. To prevent a too-low foaming ratio from affecting foam fluidity, as well as preventing a too-high foaming ratio from affecting the density and cooling effect of the foam film, the foaming ratio of the low-expansion foam extinguishing agents used in the experiment was four to seven times, and the heat flow intensity under the heat transfer mode was 15–35 kW/m² (the radiation intensity of general oil fire). According to the experimental results, the change law of thermal stability of foam extinguishing agents is expounded to guide the research and development of foam stabilizers and the efficient application of foam extinguishing agents.

2. Experimental Part

2.1. Materials

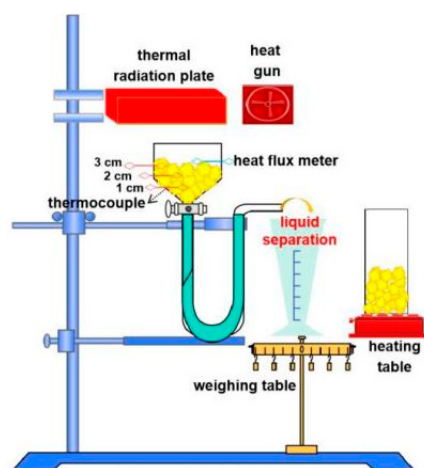
To make the research results more consistent with engineering practice, the foam fire extinguishing agents selected are all commercial foam fire extinguishing agents. The selected foams are 3% low-magnification AFFF (AF foam), a low-magnification AR foam extinguishing agent (AR foam), and a low-magnification Class A foam extinguishing agent (A foam), and the foam extinguishing agents were provided by Jiangsu Suolong Fire Technology Co., Ltd., Xinghua City, Jiangsu Province, China. The viscosity of the foam concentrate liquid of the foams was measured by rotating the No. 1 rotor of the viscometer at 60 rpm. The basic properties of the AF, AR, and A foams are provided in Table 1. The viscosity of the AF, AR, and A foams was measured by rotating the No. 21 rotor of the viscometer at 99.9 rpm. The viscosity of the AF foam is 12.2 mPa·s (torque: 24.4%), that of the AR foam is 17.1 mPa·s (torque: 34.1%), and that of the A foam is 15.4 mPa·s (torque: 30.7%).

Table 1. The basic properties of foam concentrate liquids of AF, AR, and A foams.

	Freezing Point (°C)	pH	Viscosity (mPa·s)	Surface Tension (mN/m)	Interfacial Tension (mN/m)	Diffusion Coefficient
AF	−10	7.7	4.3	17.9	2.6	4.5
AR	−10	7.6	966	19.2	3.1	2.7
A	−11	7.9	8.7	24.7	/	/

2.2. Experimental Test

To compare and study the stability of commonly used foam extinguishing agents, a foam stability test platform with three heat transfer modes was built: thermal radiation, thermal convection, and thermal conduction (Scheme 1). The measurement process of the foam effusive characteristics under thermal radiation and thermal convection was as follows: the resulting low-expansion foams were introduced into a foam funnel container, a beaker was placed at the outlet of the funnel to measure the quality of the foam effusive liquid, and then the beaker was placed on a digital balance (measuring range: 2.0 kg, accuracy: 0.01 g). The balance was connected to the computer, and the foam height in the foam container was fixed at 4 cm each time; the foaming method was compressed air, and the foaming ratio was 6–8 times. The thermal radiation source was 900 °C, and the power was 40 kW. The heat convection source was a heat gun at RT~650 °C. The position relationship between the heat radiant plate, the heat gun, and the foam layer in the experimental system was calibrated using a heat flow meter. The thermal radiation distance of the heat source was calibrated using the heat flow meter many times, and the corresponding relationship was determined (Figure S1). When the distance between the foam layer and the thermal radiation plate was 8 cm, 13 cm, and 20 cm, the heat flux intensity of the top foam layer was 35 kW/m², 25 kW/m², and 15 kW/m², respectively. To maintain consistency in wind speed, the thermal flow intensity of the foam layer at the same distance (15 cm) was regulated by regulating the temperature of the hot air gun (Figure S1b). By adjusting the temperature of the heating table, the experimental temperature (60~120 °C) of heat conduction was adjusted (Figure S1c). By adjusting the height of the foam from the heat source, the characteristics of the foaming liquid under different heat flow intensity levels were measured. The container was cleaned and dried before each repeat experiment to avoid foam residue from the last experiment affecting the next experiment. By placing the heating table and the experimental system on the balance, the change in foam evaporation quality was studied. The foam evaporation characteristics were measured by adjusting the temperature of the heating table. The balance recorded the quality change of the precipitated liquid in real time, the thermocouple recorded the temperature change of the foam layer in real time, and the digital camera recorded the shape change of the foam layer.

**Scheme 1.** Schematic diagram of experimental device for measuring foam separation and evaporation.

3. Results and Discussion

3.1. Effect of Thermal Radiation on the Foam Stability

Thermal radiation is an influential factor on the stability of foam extinguishing agents in fire. By adjusting the distance between the upper layer of a foam extinguishing agent and the heat source, the change in the liquid separation behavior of the foams under different levels of thermal radiation intensity (15 kW/m², 25 kW/m² and 35 kW/m²) was studied and is shown in Figure 1. Table 2 shows the 25% liquid separation time (t is the time taken for liquid separation; the ratio of mass/total foam mass is 25%; $t_{(i)}$, $i = 15, 25,$ and 35 shows the value of t under thermal radiation intensity levels of 15 kW/m², 25 kW/m², and 35 kW/m²), liquid separation, and evaporation percentage ($a_i = S/E$; $i = 15, 25,$ and 35 shows the value of a under thermal radiation intensity levels of 15 kW/m², 25 kW/m², and 35 kW/m²) of three kinds of foams at different thermal radiation intensities. Apparently, in the variation curve of liquid separation quality, the AF foam experiences liquid separation first, followed by the A foam and finally the AR foam extinguishing agents. With the increase in thermal radiation intensity, the time taken for the three kinds of foams to experience liquid separation also decreases, which may be due to the obvious intensification of foam evaporation under the action of the heat source, which further affects the behavior of foam separation. However, with the development of time, the mass percentage of the final liquid separation of the AF foam was significantly higher than that of the A foam and AR foam. The a_{15} , a_{25} , and a_{35} values of AR under thermal radiation heating are 1.92, 0.68, and 0.32, respectively. The a_{15} , a_{25} , and a_{35} values of the A foam under thermal convection heating are 2.69, 1.00, and 0.42, respectively. The proportion of liquid separation of the AF foam under thermal radiation heating is greater than that of AR and A, while AR possesses the relative lowest proportion of liquid separation. In the whole thermal radiation heating environment, the liquid separation behavior of the AF foam was the main behavior of foam instability. The ratio of liquid separation to evaporation mass decreased with the increase in thermal radiation intensity, but a was always greater than 1. With the increase in thermal radiation intensity, the a of AR and A foams decreased. And when the thermal radiation intensity was not less than 25 kW/m², evaporation of the AR and A foams accounted for the main behavior of foam instability.

The influence of the radiation value on the liquid separation rate of the AF, AR, and A foams is shown in Figure 2. When the initial height of the foam layer is 4 cm, it can be found that the relationship between the liquid separation rate and the radiation value is not obvious. Only when the radiation value reaches the maximum of 35 kW/m², the liquid separation rate of the solution is slightly higher than that corresponding to the other two radiation values. The results of the liquid separation rate of the AF, AR, and A foams at room temperature are shown in Figure S2. With the decrease in foam mass, the liquid separation rate of the AF, AR, and A foams decrease gradually at room temperature. The maximum liquid separation rate (LSR) of the AF foam is 0.017 g/s, that of the AR foam is 0.012 g/s, and that of the A foam is 0.005 g/s. Without the influence of thermal factors, the liquid separation rate of the AF, AR, and A foams is low. And the liquid separation of the AF foam is the fastest, followed by the AR and finally the A foams. The rate curves of the AF, AR, and A foams have similar trends when the thermal radiation intensity is 15 kW/m² and 25 kW/m². The LSR of the AF foam is 0.029 g/s at 51 s under 15 kW/m² and 0.029 g/s at 48 s under 25 kW/m². The LSR of the AR foam is 0.015 g/s at 159 s under 15 kW/m² and 0.016 g/s at 139 s under 25 kW/m². And the LSR of the A foam are 0.019 g/s at 138 s under 15 kW/m² and 0.015 g/s at 132 s under 25 kW/m². When the thermal radiation intensity is 35 kW/m², the curve of the liquid separation rate between the AF and A foams first decreases, then increases and decreases, with two extreme values and one curve peak. It may be that the AF and A foams coarsened and coalesced rapidly under high radiation intensity (35 kW/m²). The dynamic state of bubble expansion and rupture of the AF and A foams lead to a temporary increase in the rate of foam liquid separation. Moreover, under high radiation intensity (35 kW/m²), the AF and A foams quickly reached high temperatures, and the solution viscosity was at a relatively low level, which may

have also caused the increase in the foam liquid separation rate. With regard to the AR foam, there is little difference in the liquid separation curves of the foam under the three thermal radiation conditions (Figure 2b). The components of the AR foam are resistant to high temperatures, and the viscosity of the concentrated solution of the AR foam is still high after the change (using the No. 3 rotor of the rotary viscometer, the viscosity of the concentrated solution was 2389 mPa·s at 0 °C, 966 mPa·s at 20 °C, and 890 mPa·s at 50 °C). Therefore, the thermal radiation intensity has little effect on the liquid separation rate of AR foam, which is mainly related to the characteristics of AR itself. The curve of the liquid separation rate of the AR foam first increases and then decreases, and then increases and decreases, with three extreme values and two curve peaks. The LSRs of the AF and A foams at 35 kW/m² are 0.06 g/s at 38 s and 0.025 g/s at 80 s. And the LSR of the AR foam is 0.01 g/s at 151 s, which is obviously lower than that of the AF and A foams. Therefore, the liquid separation rate of the solution is related to the properties of the foam itself, such as viscosity and surface/interface tension, which are relatively independent of the external radiation heat flux of the foam [31–34].

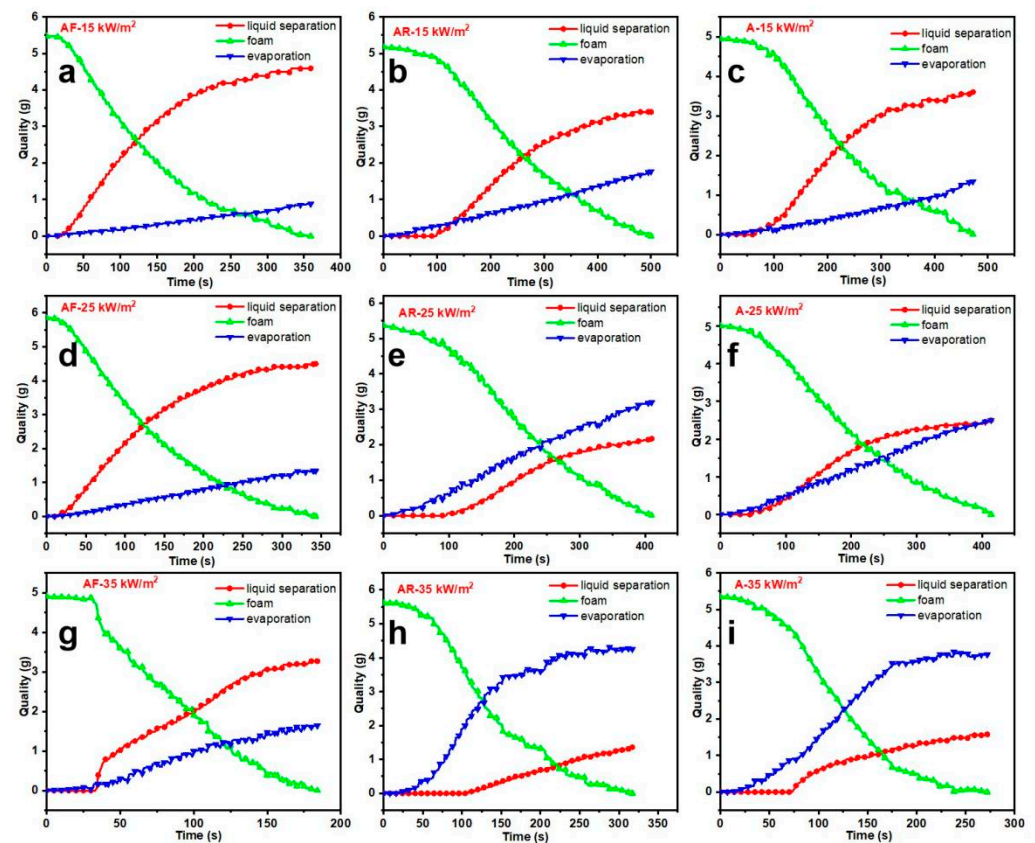


Figure 1. The foam, liquid separation quality, and evaporation curves of AF (a,d,g), AR (b,e,h), and A (c,f,i) foams under different thermal radiation intensity levels.

Table 2. The analysis of the liquid separation and evaporation quality of the foams under thermal radiation.

	$t_{(15)}$ (s)	$t_{(25)}$ (s)	$t_{(35)}$ (s)	a_{15}	a_{25}	a_{35}
AF	$71^{+0.72}_{-0.30}$	$64^{+0.45}_{-0.15}$	$64^{+0.62}_{-0.29}$	$5.20^{+0.012}_{-0.008}$	$3.35^{+0.009}_{-0.003}$	$2.00^{+0.013}_{-0.007}$
AR	$191^{+0.82}_{-0.65}$	$222^{+0.92}_{-0.72}$	$228^{+0.95}_{-0.26}$	$1.92^{+0.003}_{-0.007}$	$0.68^{+0.001}_{-0.003}$	$0.32^{+0.004}_{-0.005}$
A	$136^{+0.33}_{-0.63}$	$158^{+0.83}_{-0.51}$	$197^{+0.18}_{-0.64}$	$2.69^{+0.008}_{-0.003}$	$1.00^{+0.010}_{-0.004}$	$0.42^{+0.008}_{-0.022}$

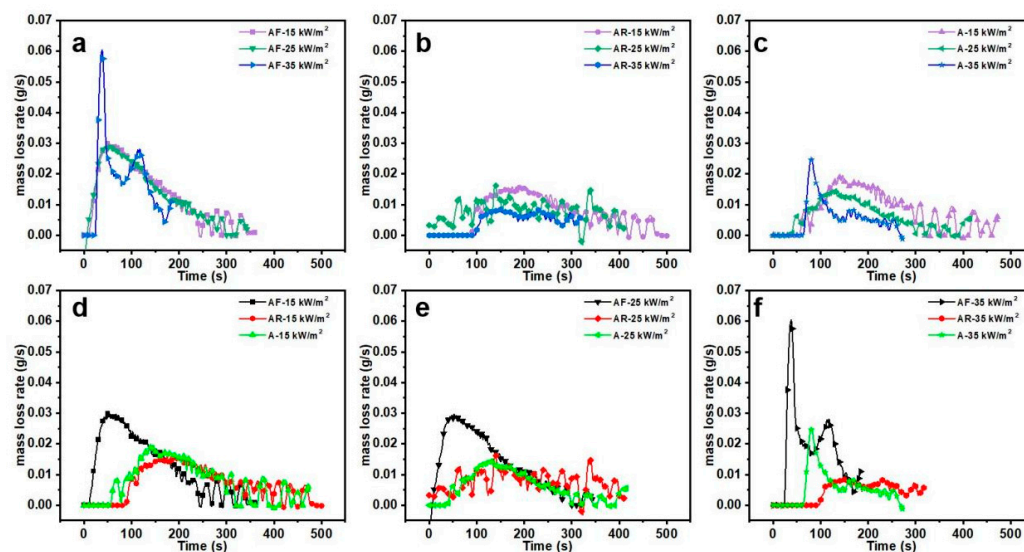


Figure 2. The mass loss rate (liquid separation quality) curves of AF, AR, and A foams (a–f) under different thermal radiation intensity levels.

To further discuss the behavior of foam liquid separation, the temperature analysis results of the foam layer are shown in Figure 3. The initial height of the foam layer is 4 cm, and thermocouples are placed at foam layer heights of 1 cm, 2 cm, and 3 cm (distance from bottom of foam layer) to study the temperature change of the foam layer heated by thermal radiation. Under the condition of radiation heating, the foam will expand, merge, and burst, so the foam mass loss mainly has two parts: foam liquid separation and evaporation. The temperature change trend of the foam layer in three places is the same, and the foam at 3 cm first reaches about 90 °C; then, the foam bursts, the thermocouple leaks into the air, and the temperature rises. In this experiment, the behavior of the liquid separation of foams is mainly studied. In Figure 3, the internal temperature of the AF, AR, and A foams in the thermal radiation layer stabilized at about 30 °C in the initial stage of heating. And then the foam layer was heated continuously, which led to the high expansion of the foams, and the temperature of the foam layer quickly rose to 90 °C. In the time range from the beginning of the experiment to the last 100 s, the foam liquid dissolution rate and evaporation rate were faster. In addition, when all bubbles were close to 100 °C at the end of the experiment, the viscosity of the AF and A solutions was at the lowest level, which may have also led to the increase in the liquid separation rate of the AF and A foams at 35 kW/m².

The heights of the three kinds of foams have the same variation tendency: the foam expands first and then contracts. In the initial stage of thermal radiation heating, due to the expansion of gas molecules in the foams, the foam height increases. Then, the foams continue to be affected by external thermal radiation, the liquid in the foam rapidly discharges, and the foam begins to burst and collapse, when the height gradually drops. Under the conditions of 15 kW/m² and 25 kW/m², the liquid separation rate of the three kinds of foam echoes the changing trend of foam height. Because it takes time to detect the quality of the foam liquid separation device, the liquid separation rate curve lags behind the foam height curve in Figure 3a–f. There is a waiting time for the solution to experience liquid separation, and the reason for the waiting time is mainly because there will be a re-integration stage of the overall structure of the foam before the solution is separated out. Usually, the liquid content of the initial foam film is certain, so it will take some time for the liquid to move from the film to the Prandtl boundary.

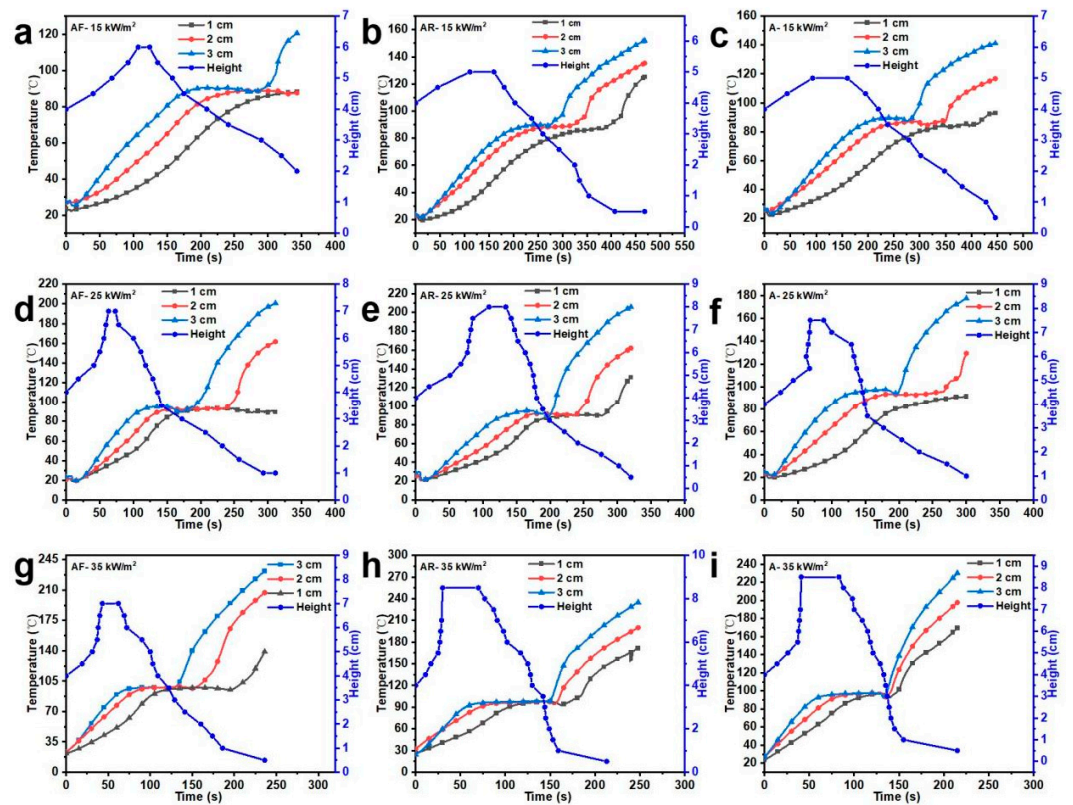


Figure 3. The temperature curves of foam layers and the height curves of AF (a,d,g), AR (b,e,h), and A (c,f,i) foams under different thermal radiation intensity levels.

In the expansion stage, the maximum heights of the AF, AR, and A foams at 15 kW/m² are 6 cm, 5 cm, and 5 cm, and the time to reach the maximum height is 107 s, 111 s, and 93 s, respectively. The maximum heights of the AF, AR, and A foams at 25 kW/m² are 7 cm, 8 cm, and 7.5 cm, and the time to reach the maximum height is 63 s, 109 s, and 68 s, respectively. The maximum heights of the AF, AR, and A foams at 35 kW/m² are 7 cm, 8.5 cm, and 8.5 cm, and the time to reach the maximum height is 43 s, 30 s, and 41 s, respectively. It can be seen that with the increase in the thermal radiation intensity, the expansion height of the AR and A foams increases more than that of AF. This is because in the initial stage of heating, the additives in the AR and A foams can improve the stability of the foams, which is beneficial for foam expansion. Moreover, the height attenuation of the AR and AF foams at 15 kW/m² and 25 kW/m² is slow under heating radiation; that is, their thermal stability is better.

3.2. Effect of Thermal Convection on the Foam Stability

By adjusting the distance between the hot air gun and the foam sample, the influence of the thermal convection intensity (15 kW/m², 25 kW/m², and 35 kW/m²) on the foam stability was studied and is shown in Table 3 and Figures 4–6. With the increase in the thermal convection intensity, the 25% liquid separation time of the three foams decreased. Similarly, the t of AR is longer than that of the A and AF foams. AF foam has the lowest t value and the fastest liquid separation time (Figure 4). Specially, the $t_{(15)}$ values of AF, AR, and A foams are 87 s, 298 s, and 106 s, respectively. In the whole thermal convection heating environment, the liquid separation behavior of AF foam is the main behavior of foam instability. The ratio of liquid separation to evaporation mass decreases with the increase in thermal radiation intensity, but a is always greater than 2, which means that under convection heating, the proportion of liquid separation in AF foam is higher than that of evaporation. When the heat flux intensity is 15 kW/m² and 25 kW/m², the a_{15} and a_{25} values of AF under thermal convection heating are 3.03 and 2.81, respectively, which

are lower than that of AF foam under thermal radiation heating (5.2 and 3.35). That is, the proportion of AF foam precipitation under thermal radiation heating is higher than that under thermal convection heating when the heat flux intensity is 15 kW/m² and 25 kW/m². With the increase in thermal radiation intensity, the *a* of AR and A foams decreases. The *a*₁₅, *a*₂₅, and *a*₃₅ values of AR under thermal convection heating are 3.98, 3.17, and 2.46, respectively, which are higher than those of AR foam under thermal radiation heating (1.92, 0.68, and 0.32). The *a*₁₅, *a*₂₅, and *a*₃₅ values of the A foam under thermal convection heating are 6.26, 5.78, and 3.74, respectively, which are higher than those of the A foam under thermal radiation heating (2.69, 1.00, and 0.42). It can be seen that, different from the AF foam, the ratio of liquid separation under thermal convection of the AR and A foams is higher than that under thermal radiation heating. Different from the case of thermal radiation heating, the proportion of liquid separation of the A foam under thermal convection heating is greater than that of AR and AF, while AF possesses the relative lowest proportion of liquid separation.

Table 3. The analysis of the liquid separation and evaporation quality of the foams under thermal convection.

	<i>t</i> ₍₁₅₎ (s)	<i>t</i> ₍₂₅₎ (s)	<i>t</i> ₍₃₅₎ (s)	<i>a</i> ₁₅	<i>a</i> ₂₅	<i>a</i> ₃₅
AF	87 ^{+0.54} −0.51	83 ^{+0.35} −0.22	78 ^{+0.77} −0.13	3.03 ^{+0.003} −0.001	2.81 ^{+0.003} −0.005	2.78 ^{+0.007} −0.002
AR	298 ^{+0.12} −0.49	254 ^{+0.66} −0.15	225 ^{+0.14} −0.53	3.98 ^{+0.010} −0.007	3.17 ^{+0.009} −0.015	2.46 ^{+0.003} −0.004
A	106 ^{+0.73} −0.55	102 ^{+0.58} −0.27	98 ^{+0.28} −0.30	6.26 ^{+0.006} −0.011	5.78 ^{+0.004} −0.002	3.74 ^{+0.001} −0.005

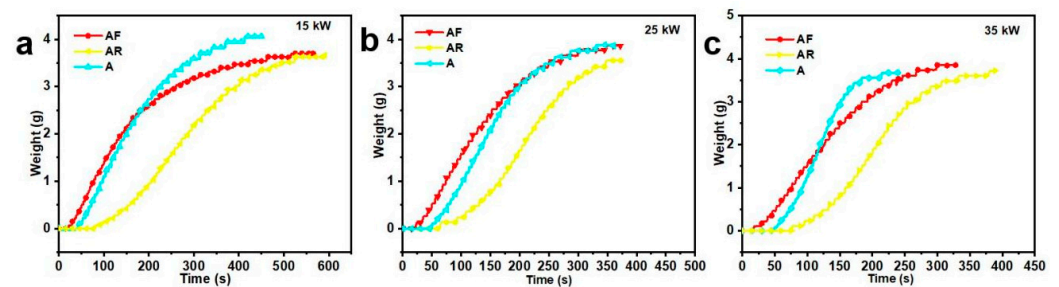


Figure 4. The liquid separation quality curves of AF, AR, and A foams (a–c) at different thermal convection intensity levels.

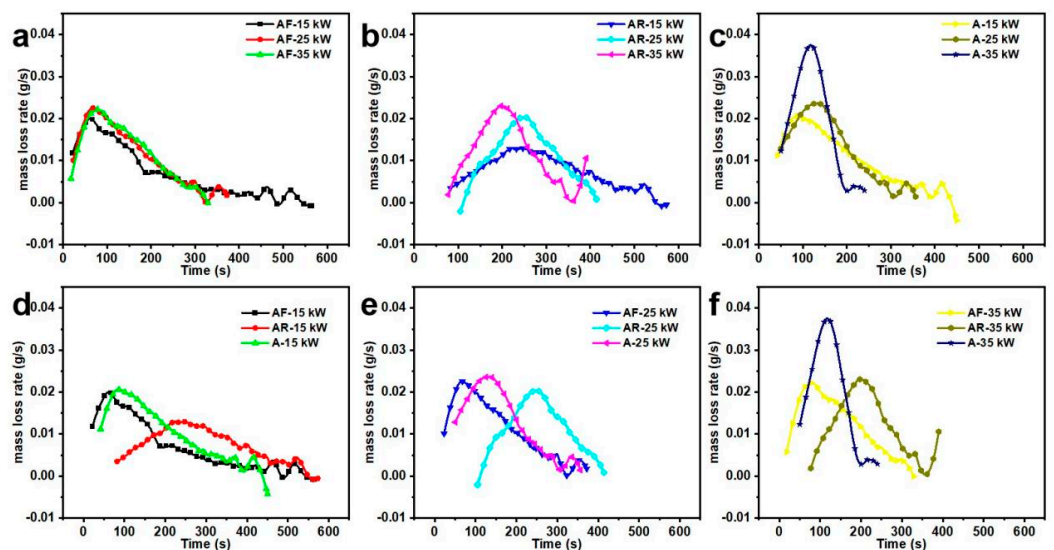


Figure 5. The mass loss rate (liquid separation quality) curves of AF, AR, and A foams (a–f) under different thermal convection intensity levels.

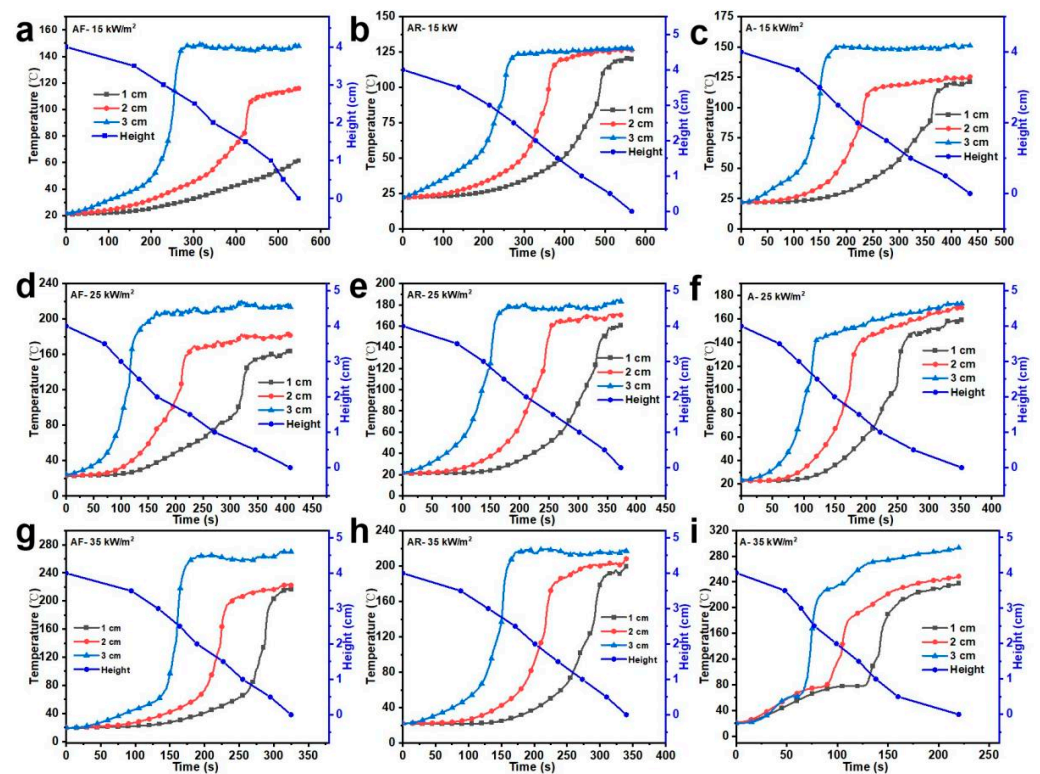


Figure 6. The temperature curves of foam layers and the height curves of AF (a,d,g), AR (b,e,h), and A (c,f,i) foams under different thermal convection intensity levels.

The mass loss behavior of the three foams at different levels of thermal convection intensity is studied in Figures 5 and 6. With the increase in time, the liquid separation rate of AF, AR, and A foams first increases and then decreases. The liquid separation behavior of AF foam occurs first, followed by that of the A foam, and the time to begin liquid separation of the AR foam is the slowest. The LSR of the AF foam is 0.020 g/s at 61 s under 15 kW/m², 0.022 g/s at 67 s under 25 kW/m², and 0.022 g/s at 78 s under 35 kW/m². The LSR of the AR foam is 0.012 g/s at 239 s under 15 kW/m², 0.020 g/s at 250 s under 25 kW/m², and 0.023 g/s at 198 s under 35 kW/m². The LSR of the A foam is the largest, which may be due to the fact that with the increase in the foam layer temperature, the viscosity of the A foam decreased more than that of the AF and AR foams, and the liquid separation rate was higher than that of the AF foam and AR foam. In addition, when all bubbles were close to 100 °C, the viscosity of the solution was at the lowest level, which may have also led to the increase in the liquid separation rate of the foam, as shown in Figure 5b. Under thermal convection, the thermal stability of AR foam is better than that of A and AF foams. Under thermal convection, the lower thermal radiation intensity (15 kW/m², 25 kW/m²) has little effect on the liquid separation rate of AF and A foams, which is similar to results under thermal radiation conditions, but has a great effect on AR foam. Different from the result in Figure 2b, after the superposition of the dynamic influence of wind and the thermodynamic influence of heat, the liquid separation rate of AR foam at 25 kW/m² and 35 kW/m² is higher than that of AR at 15 kW/m² (Figure 5b,e). This may be due to the dynamic coalescence and coarsening of AR foam under the influence of hot air power. Therefore, both the thermal environment and external power will affect the liquid separation behavior of foam [25,35–37].

The temperature changes of the foam layer under thermal convection are shown in Figure 6. Different from the thermal radiation experiment, the height of the three kinds of foam layers decreases under the influence of thermal convection, which is mainly due to the slow temperature rise of the foam layer under hot air in thermal convection, and the foam directly breaks the wall and then precipitates. The thermocouple in the foam

layer was completely exposed to the air as the height of the foam layer decreased, and the air temperature began to be measured. Under the constant heating of thermal convection, the thermocouple temperature continued to rise until it reached the thermal equilibrium temperature in Figure 6.

As can be seen from Figure 6a,d,g, the liquid separation rate of AF foam is faster; the height of the foam layer drops rapidly. The temperatures of the foam layer at 1 cm, 2 cm, and 3 cm of the AF foam under 15 kW/m^2 are $51 \text{ }^\circ\text{C}$, $55.2 \text{ }^\circ\text{C}$, and $66.6 \text{ }^\circ\text{C}$, respectively. The temperatures of the foam layer at 1 cm, 2 cm, and 3 cm of the AR foam under 15 kW/m^2 are $66.8 \text{ }^\circ\text{C}$, $68.2 \text{ }^\circ\text{C}$, and $65.5 \text{ }^\circ\text{C}$, respectively. The temperatures of the foam layer at 1 cm, 2 cm, and 3 cm of the A foam under 15 kW/m^2 are $70.1 \text{ }^\circ\text{C}$, $79.8 \text{ }^\circ\text{C}$, and $111.4 \text{ }^\circ\text{C}$, respectively. Compared with the temperatures of the foam layer of the three kinds foams (near $90 \text{ }^\circ\text{C}$) under thermal radiation of 15 kW/m^2 in Figure 3, the temperatures of the foam layer of the three kinds foams under thermal convection of 15 kW/m^2 are lower, which is mainly due to the accelerated heat exchange of the foam layer under thermal convection, as well as the obvious increase in foam evaporation, cracking, and heat absorption. Under the heat convection of 15 kW/m^2 , the foam layer temperature of the A foam is higher than that of AR and AF. The temperatures of the foam layer at 1 cm, 2 cm, and 3 cm of the AF foam under 35 kW/m^2 are $65.3 \text{ }^\circ\text{C}$, $60.6 \text{ }^\circ\text{C}$, and $62.2 \text{ }^\circ\text{C}$, respectively. The temperature of the foam layer at 1 cm, 2 cm, and 3 cm of the AR foam under 35 kW/m^2 are $108.5 \text{ }^\circ\text{C}$, $93.1 \text{ }^\circ\text{C}$, and $83.0 \text{ }^\circ\text{C}$, respectively. The temperature of the foam layer at 1 cm, 2 cm, and 3 cm of the A foam under 35 kW/m^2 are $121.9 \text{ }^\circ\text{C}$, $109.5 \text{ }^\circ\text{C}$, and $65.9 \text{ }^\circ\text{C}$, respectively. Due to the excellent rapid liquid separation behavior of AF, the thermal convection intensity is 35 kW/m^2 , and the temperature of the AF foam layer is still below $100 \text{ }^\circ\text{C}$. The final temperature of the AR and A foam layers was higher than $100 \text{ }^\circ\text{C}$, mainly because the foam had been completely eluted under continuous heating. Under the continuous heating of thermal convection, the foam layer continues to evaporate at a high height, forming a steam mixture, resulting in the foam layer temperature being higher than $100 \text{ }^\circ\text{C}$. This further shows that the thermal stability of the AR and A foams is also higher than that of the AF foam under the influence of thermal convection, but the cooling effect of the AF foam is better than that of the AR and A foams.

3.3. Effect of Thermal Conduction on the Foam Stability

By adjusting the temperature of the bottom heat source, the thermal stability of low-magnification foam at different heat conduction temperatures was studied. The changes in the evaporation quality of the three kinds of foam extinguishing agents when the heat source exceeds $100 \text{ }^\circ\text{C}$ are shown in Figure 7. With the increase in the temperature of the heat source at the bottom of the foam extinguishing agent, the liquid separation rate of the three foam extinguishing agents is obviously improved, and finally, the quality of the separated liquid is improved. Compared with AR and AF foam extinguishing agents, the low-power A foam extinguishing agent is the first to evaporate. At the initial stage, the evaporation rate of A foam was significantly higher than that of the AR and AF foams, and the possible reason was that the viscosity of the AR and AF foams was higher than that of the A foam. AF foam has the lowest evaporation rate and the longest retention time of foam morphology. The quality of liquid precipitated after the foam morphology is completely broken is the least. AF foam has the lowest evaporation rate and the longest retention time of foam morphology. The quality of liquid precipitated after its foam morphology is completely broken is the lowest. The main reason is that AF foam quickly precipitates liquid, the liquid evaporates and bubbles under the constant heating of the bottom heat source, and the evaporation rate is further improved. The middle layer of the AF foam was hollowed out first, and the upper layer of the foam had little direct contact with heat source, and remained in foam form for a long time. In Figure 7a,b,d,e, the evaporation rate in the early stage of AR is similar to that of AF (time before 400 s).

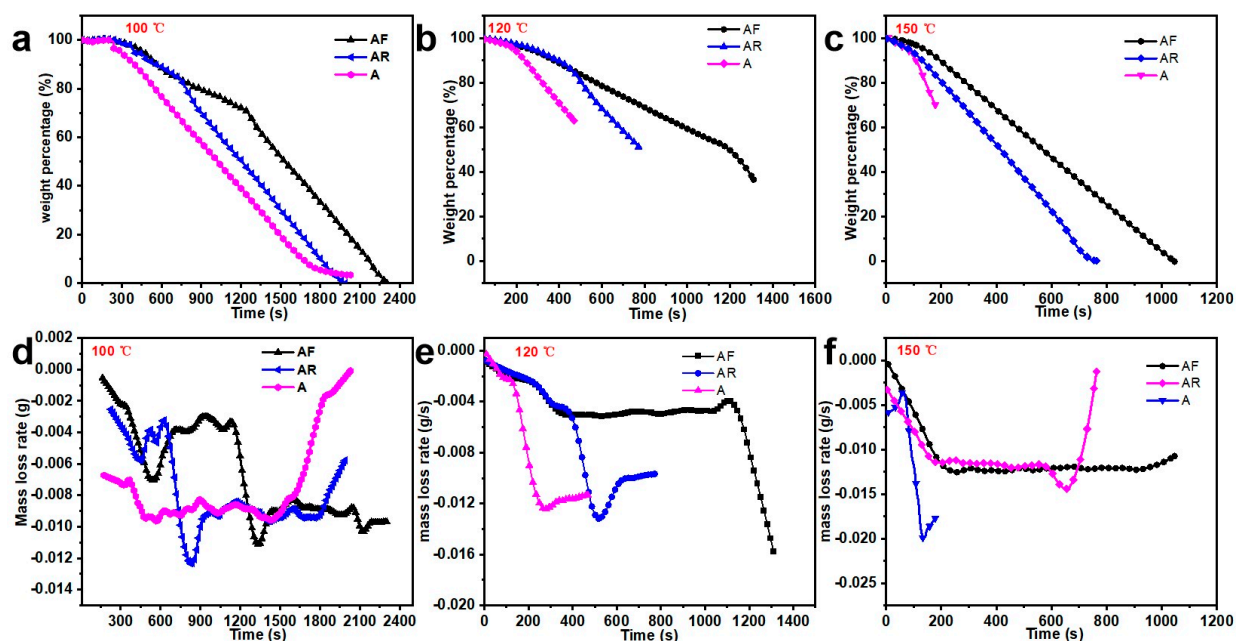


Figure 7. The evaporation quality curves (a–c) and the mass loss rate (evaporation quality) curves (d–f) of AF, AR, and A foams under different thermal conduction intensity levels.

The mass change rate, that is, the evaporation rate of foam, changes with time, as shown in Figure 8. With the temperature increasing, the evaporation rate of AF foam is larger than that of the AR and A foams. The evaporation rate of A foam increases with the temperature. The micro-morphology of the three kinds of foams at room temperature was recorded using an optical microscope, and the average particle size of the three kinds of foam was studied. The average particle size of the AF, AR, and A foams at room temperature, 40 °C, and 60 °C is shown in Figure S3. With the increase in time and temperature, all three kinds of foam coalesce and coarsen, and the average particle size of the foams increases (Figure S3). Among them, the average particle size of AF is the smallest at room temperature, and with the increase in temperature, the coarsening rate of the AF particle size is obviously higher than that of the AR and A foams. The coarsening rate of the AR and A foams is equivalent. The A foam extinguishing agent experienced liquid separation quickly, and the time of maintaining the extinguishing agent in foam form was obviously shorter than that of the AF and AR foam extinguishants, which may be related to the different viscosity and average foam particle size of the three foams (Table 1 and Figure S3).

The temperature changes of the three foams' layers were investigated, and the results of the foam layers under heat conduction at 100 °C and 150 °C are shown in Figure 9. The initial height of the foam layer was 4 cm, and thermocouples were placed at the foam layer heights of 1 cm, 2 cm, and 3 cm to study the temperature change of the foam layer heated by thermal conduction. Under the condition of thermal conduction, the foam will expand, merge, and burst, so the foam mass loss mainly has two parts: liquid separation and evaporation. The temperature change trend of the foam layer in three places is the same, and the foam layer at 1 cm (close to heat source) first reaches about 90 °C; then, the foam bursts, the thermocouple leaks into the air, and the temperature rises and maintains the temperature of thermal equilibrium. When the temperature of the AF foam layer reaches 100 °C, a lot of foam is broken and liquid is precipitated, and the proportion of liquid precipitation decreases with the increase in the heat conduction temperature. The evaporation rate of the AF foam is also slightly higher than that of the AR and A foams (Figure 7). Under heat conduction, AF quickly experiences liquid separation and evaporation, which causes the temperature of the AF foam layer to rise at a lower rate than

that of the AR and A foams. That is, in a thermal environment, the cooling effect of the AF foam is better than that of the AR and A foams.

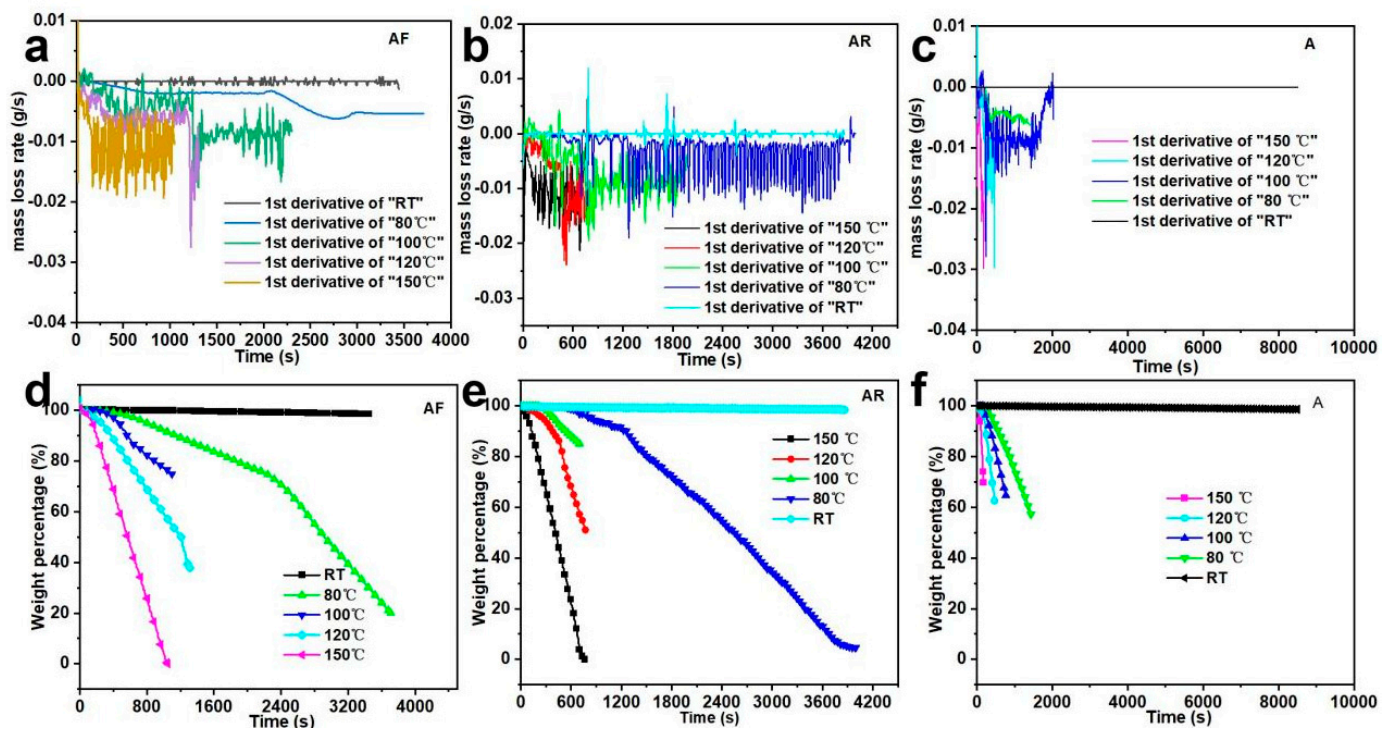


Figure 8. The evaporation rate analysis of AF (a,d),AR (b,e),and A (c,f) foams under different thermal conduction intensity levels.

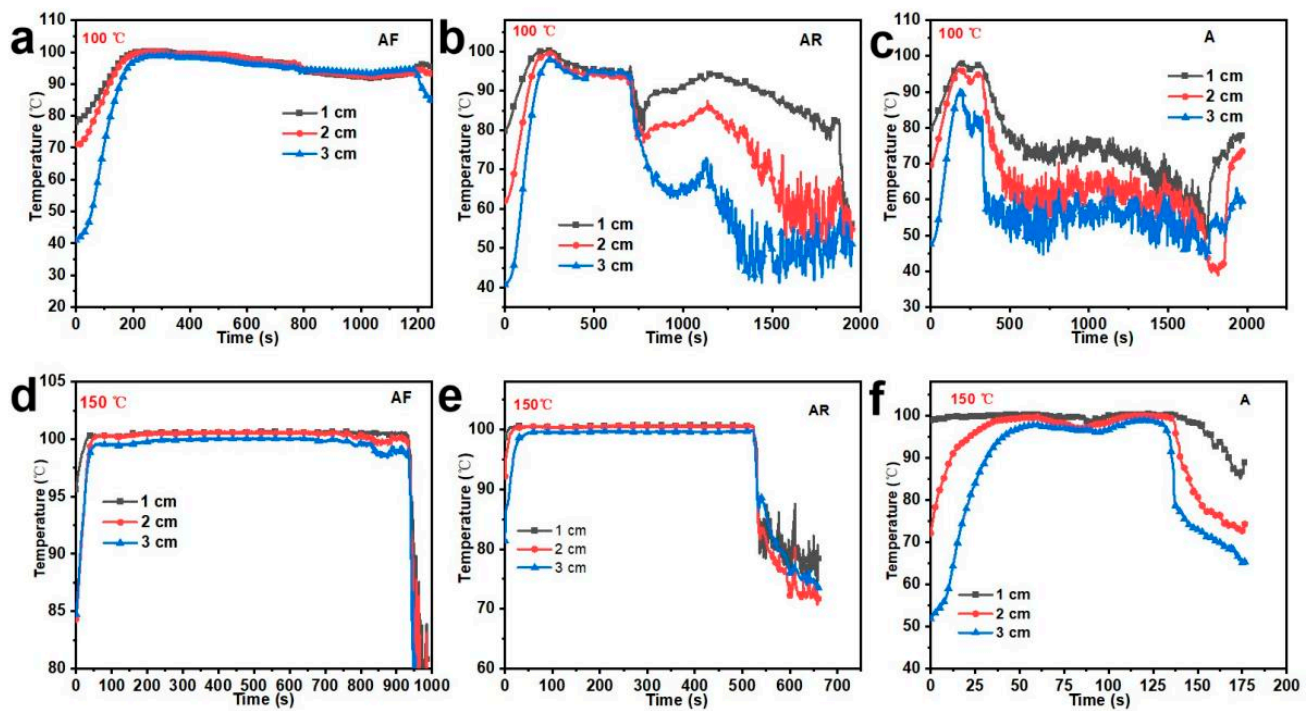


Figure 9. The temperature curves of foam layers of AF (a,d), AR (b,e) and A (c,f) foams under different thermal conduction intensity levels.

4. Conclusions

By studying the characteristic liquid separation and evaporation behaviors of AF, AR, and A foams under different heat transfer modes, the thermal stability of the foams in a thermal environment was analyzed. At a relatively low thermal radiation intensity, the liquid separation rate of the AF, AR, and A foams is related to the properties of the foam itself, such as viscosity and surface/interface tension, which is relatively independent of the external radiation heat flux of the foam. Under low radiation intensity (15 kW/m² and 25 kW/m²), the liquid separation rate of AF and A foams is relatively stable. When the heat flux intensity is 35 kW/m², the liquid separation rate of AF and A foams increases notably, which may be mainly due to the rapid decrease in foam viscosity. Under the condition of thermal radiation heating, the precipitation rate of AR is relatively stable, and the high viscosity of AR is the main reason for this. However, under the condition of thermal convection heating, the precipitation rate of AR is notably improved. At this time, under the influence of wind power, the rapid aggregation and coarsening of AR is the main reason. Therefore, both the thermal environment and external power will affect the liquid separation behavior of foam. As evaporation is mainly dominated by the liquid phase transformation of the foam liquid, there is no significant difference in the evaporation rates of the three kinds of foam under the same heat conduction condition. The foam survival time of AF and AR foams is longer, which may be due to the fact that the foam is formed again by blowing air under the action of the heat source after AF and AR's rapid liquid dissolution. In addition, AR and A foams usually have a larger t value under thermal radiation and thermal convection, and their thermal stability is better than that of AF foam. The temperature reached by the AF foam layer under heat convection is lower than that of AR and A foams, and the time for the foam layer to reach the highest temperature under thermal conduction is longer than that of AR and A foams, which indicates that the cooling effect of AF foam is better than that of AR and A foams. Therefore, AR and A foams can be used for thermal insulation protection, and AF foam can be used for rapid fire suppression and cooling.

Supplementary Materials: The following supporting information can be downloaded at: <https://www.mdpi.com/article/10.3390/fire7040137/s1>. Figure S1: calibration results of heat flux intensity and heat conduction temperature; Figure S2: liquid separation rate curves of AF, AR and A foams at room temperature; Figure S3: average particle size of AF, AR and A foams at room temperature (RT), 40 °C and 60 °C.

Author Contributions: Conceptualization, data curation, formal analysis, investigation, methodology, writing—original draft, project administration, resources, funding acquisition, X.Z.; Data curation, formal analysis, investigation, writing—review & editing, Z.A., Z.L., H.H. and Y.L.; visualization, supervision, project administration, funding acquisition, R.P. All authors have read and agreed to the published version of the manuscript.

Funding: This research was funded by the National Key R&D Program of China (No.2022YFC3004901), the Program of Tianjin Science and Technology Plan (22JCQNJC01740), the Natural Science Foundation of Jiangsu Province (Grants No.BK20230943), the Hongkong Scholar Program (XJ2023051). The APC was funded by No.2022YFC3004901.

Institutional Review Board Statement: Not applicable.

Informed Consent Statement: Not applicable.

Data Availability Statement: The data that support the findings of this study are available on request from the corresponding author, [X.Z.], upon reasonable request.

Conflicts of Interest: The authors declare no competing financial interests.

References

1. Deng, T.; Liu, C.; Huang, L.; Shen, J. Research progress of positive pressure foam extinguishing technology. *China Saf. Sci. J. (CSSJ)* **2019**, *29*, 64–70.
2. Hu, B.; Liu, F.; Zhang, R.; Yang, G.; Lu, J.; Wu, L. Environmental performance assessment for foam extinguishing agent and research progress. *Environ. Prot. Chem. Ind.* **2020**, *40*, 573–579.
3. Yuan, S.; Chang, C.; Yan, S.; Zhou, P.; Qian, X.; Yuan, M.; Liu, K. A review of fire-extinguishing agent on suppressing lithium-ion batteries fire. *J. Energy Chem.* **2021**, *62*, 262–280. [[CrossRef](#)]
4. Zhang, Y.; Tian, Z.; Ye, Q.; Lu, Y. Research progress of gel foam extinguishing agent in coal mines. *Fire* **2023**, *6*, 470. [[CrossRef](#)]
5. Shi, Q.; Yang, H.; Li, H. Research on preparation of film-forming colloidal foam and its fire extinguishing and cooling characteristics. *China Saf. Sci. J. (CSSJ)* **2022**, *32*, 121–126.
6. Wang, X.; Liao, Y.; Lin, L. Experimental study on fire extinguishing with a newly prepared multi-component compressed air foam. *Chin. Sci. Bull.* **2009**, *54*, 492–496. [[CrossRef](#)]
7. Wu, L.; Liu, M.; Zhang, M.; Zhang, J.; Wang, Z.; Jing, W.; Zhu, X. Effect of aqueous film-forming foaming agent on liquid drops cooling on high-temperature metal surface. *J. Saf. Environ.* **2023**, *23*, 1880–1888.
8. Wu, L.; Zhang, J.; Ma, Z.; Zhang, M.; Zhang, X.; Yan, Q.; Wang, C. Thermal aging mechanisms of foam fire extinguishing agents. *J. Beijing Univ. Chem. Technol. Nat. Sci. Ed.* **2022**, *49*, 48–55.
9. Simjoo, M.; Rezaei, T.; Andrianov, A.; Zitha, P.L.J. Foam stability in the presence of oil: Effect of surfactant concentration and oil type. *Colloids Surf. A Physicochem. Eng. Asp.* **2013**, *438*, 148–158. [[CrossRef](#)]
10. Osei-Bonsu, K.; Shokri, N.; Grassia, P. Foam stability in the presence and absence of hydrocarbons: From bubble- to bulk-scale. *Colloids Surf. A Physicochem. Eng. Asp.* **2015**, *481*, 514–526. [[CrossRef](#)]
11. An, N.; Qiao, J.-J. Study of high performance alcohol-resistance foam extinguishing agent. *J. East China Univ. Sci. Technol. (Nat. Sci. Ed.)* **2018**, *44*, 75–81.
12. Hu, B.; Su, Z.; Pan, X.; Chen, Y.; Lang, X. Experimental study on the efficiency of hydrocarbon pool fire extinguishment based on AFFF superimposition method. *J. Saf. Environ.* **2023**, *23*, 2296–2303.
13. Liu, H.; Duan, J.; Jiang, X.; Zhai, Y.; Wang, Y.; Wang, D. Experimental probe on the thermal stability of the 3-phase foam extinguishing agent. *J. Saf. Environ.* **2019**, *19*, 502–508.
14. Li, X.; Guo, R.; Qian, X. Research on the influence of wollastonite fibers on the stability of foam extinguishment agent and its effect on the extinguishing efficiency of pool fire. *Fire Mater.* **2020**, *44*, 1053–1063. [[CrossRef](#)]
15. Ponomarenko, R.; Loboichenko, V.; Strelets, V.; Gurbanova, M.; Morozov, A.; Kovalov, P.; Shevchenko, R.; Kovalova, T. Review of the environmental characteristics of fire extinguishing substances of different composition used for fires extinguishing of various classes. *J. Eng. Appl. Sci.* **2019**, *14*, 5925–5941.
16. Ranjani, I.S.; Ramamurthy, K. Relative assessment of density and stability of foam produced with four synthetic surfactants. *Mater. Struct.* **2010**, *43*, 1317–1325. [[CrossRef](#)]
17. Sheng, Y.; Wu, X.; Lu, S.; Li, C. Experimental study on foam properties of mixed systems of silicone and hydrocarbon surfactants. *J. Surfactants Deterg.* **2016**, *19*, 823–831. [[CrossRef](#)]
18. Sheng, Y.; Xue, M.; Zhang, S.; Wang, Y.; Zhai, X.; Zhao, Y.; Ma, L.; Liu, X. Role of nanoparticles in the performance of foam stabilized by a mixture of hydrocarbon and fluorocarbon surfactants. *Chem. Eng. Sci.* **2020**, *228*, 115977. [[CrossRef](#)]
19. Li, H.; Yu, X.; Qiu, K.; Bo, B.; Li, Q.; Lu, S. Role of salts in fire extinguishing performance of aqueous film-forming foam (AFFF). *Case Stud. Therm. Eng.* **2023**, *49*, 103159. [[CrossRef](#)]
20. Babamahmoudi, S.; Riahi, S. Application of nano particle for enhancement of foam stability in the presence of crude oil: Experimental investigation. *J. Mol. Liq.* **2018**, *264*, 499–509. [[CrossRef](#)]
21. Yu, X.; Jiang, N.; Miao, X.; Li, F.; Wang, J.; Zong, R.; Lu, S. Comparative studies on foam stability, oil-film interaction and fire extinguishing performance for fluorine-free and fluorinated foams. *Process Saf. Environ. Prot. Chem. Ind.* **2020**, *133*, 201–215. [[CrossRef](#)]
22. Yu, X.; Lin, Y.; Li, F.; Yu, X.; Li, H.; Zong, R.; Lu, S. Highly stable fluorine-free foam by synergistically combining hydrolyzed rice protein and ferrous sulfate. *Chem. Eng. Sci.* **2022**, *250*, 117378. [[CrossRef](#)]
23. Kong, D.; Wang, D.; Chen, J.; Zhang, J.; He, X.; Li, B.; He, X.; Liu, H. Assessing the mixed foam stability of different foam extinguishing agents under room temperature and thermal radiation: An experimental study. *J. Mol. Liq.* **2023**, *369*, 120805. [[CrossRef](#)]
24. Sheng, Y.; Lu, S.; Jiang, N.; Wu, X.; Li, C. Drainage of aqueous film-forming foam stabilized by different foam stabilizers. *J. Dispers. Sci. Technol.* **2018**, *39*, 1266–1273. [[CrossRef](#)]
25. Li, Q.; Qiu, K.; Li, C.; Li, H.; Zhang, M.; Liu, H. Stability and rheological properties of firefighting foams with sodium carboxymethyl cellulose and hydrocarbon/silicone surfactants. *Chem. Eng. Sci.* **2024**, *288*, 119733. [[CrossRef](#)]
26. Zhu, J.; Zheng, N.; Yang, Z.; Li, X.; Lei, T. Experimental study on the foam-stabilizing advantages and foam stabilization mechanism of novel microbial polysaccharides. *J. Mol. Liq.* **2023**, *385*, 122428. [[CrossRef](#)]
27. Oetjen, K.; Bilke-Krause, C.; Madani, M.; Willers, T. Temperature effect on foamability, foam stability, and foam structure of milk. *Colloids Surf. A Physicochem. Eng. Asp.* **2014**, *460*, 280–285. [[CrossRef](#)]
28. Yekeen, N.; Idris, A.K.; Manan, M.A.; Samin, A.M.; Risal, A.R.; Kun, T.X. Bulk and bubble-scale experimental studies of influence of nanoparticles on foam stability. *Chin. J. Chem. Eng.* **2017**, *25*, 347–357. [[CrossRef](#)]

29. Lunkenheimer, K.; Malysa, K.; Winsel, K.; Geggel, K.; Siegel, S. Novel Method and Parameters for Testing and Characterization of Foam Stability. *Langmuir* **2010**, *26*, 3883–3888. [[CrossRef](#)]
30. Magrabi, S.A.; Dlugogorski, B.Z.; Jameson, G.J. A comparative study of drainage characteristics in AFFF and FFFP compressed-air fire-fighting foams. *Fire Saf. J.* **2002**, *37*, 21–52. [[CrossRef](#)]
31. Zhou, R.; Lang, X.; Zhang, X.; Tao, B.; He, L. Thermal stability and insulation characteristics of three-phase fire-fighting foam exposed to radiant heating. *Process Saf. Environ. Prot.* **2021**, *146*, 360–368. [[CrossRef](#)]
32. Yu, X.; Yu, X.; Lin, Y.; Li, H.; Li, G.; Zong, R. Comparative study on interfacial properties, foam stability, and firefighting performance of c6 fluorocarbon surfactants with different hydrophilic groups. *Langmuir* **2023**, *39*, 16336–16348. [[CrossRef](#)] [[PubMed](#)]
33. Sheng, Y.; Peng, Y.; Zhang, S.; Guo, Y.; Ma, L.; Zhang, H. Thermal stability of foams stabilized by fluorocarbon and hydrocarbon surfactants in presence of nanoparticles with different specific surface areas. *J. Mol. Liq.* **2022**, *365*, 120187. [[CrossRef](#)]
34. Sheng, Y.; Peng, Y.; Zhang, S.; Guo, Y.; Ma, L.; Wang, Q.; Zhang, H. Study on thermal stability of gel foam co-stabilized by hydrophilic silica nanoparticles and surfactants. *Gels* **2022**, *8*, 123. [[CrossRef](#)] [[PubMed](#)]
35. Wang, L.; Zhu, W.; Qian, Y. Interface characteristics and stability mechanisms of bubbles in high-concentration bentonite slurry. *J. Mol. Liq.* **2023**, *387*, 122602. [[CrossRef](#)]
36. Wang, H.; Wang, Z.; Lv, Q.; Li, C.; Du, Z.; Sun, S.; Hu, S. Mechanism of foam film destruction induced by emulsified oil: A coarse-grained simulation study. *J. Phys. Chem. C* **2018**, *122*, 26438–26446. [[CrossRef](#)]
37. Ping, P.; Li, B.; Chen, J.; He, X.; Wang, D.; Zhang, J.; Kong, D. Effect of temperature on stability and film thinning behavior of aqueous film forming foam. *J. Mol. Liq.* **2023**, *370*, 120978. [[CrossRef](#)]

Disclaimer/Publisher’s Note: The statements, opinions and data contained in all publications are solely those of the individual author(s) and contributor(s) and not of MDPI and/or the editor(s). MDPI and/or the editor(s) disclaim responsibility for any injury to people or property resulting from any ideas, methods, instructions or products referred to in the content.